NMR Studies on Solution Structures of Methanol and Ethanol Saturated with CO2

ARTICLE *in* JOURNAL OF SOLUTION CHEMISTRY · NOVEMBER 2014

Impact Factor: 1.18 · DOI: 10.1007/s10953-014-0222-z

6 AUTHORS, INCLUDING:

Toshiyuki Takamuku
Saga University
84 PUBLICATIONS **1,916** CITATIONS
SEE PROFILE

Takashi Makino
National Institute of Advanc…
42 PUBLICATIONS **349** CITATIONS
SEE PROFILE

J Solution Chem (2014) 43:1539–1549
DOI 10.1007/s10953-014-0222-z

NMR Studies on Solution Structures of Methanol and Ethanol Saturated with CO_2

T. Umecky · T. Takamuku · T. Aida · T. Makino · T. Aizawa · M. Kanakubo

Received: 17 November 2013 / Accepted: 28 January 2014 / Published online: 20 September 2014

Abstract ^{2}H and ^{17}O NMR relaxation times, $T_1(^2\text{H})$ and $T_1(^{17}\text{O})$, and ^{2}H NMR chemical shifts, $\delta(^2\text{H})$, in CO_2-saturated CD_3OD and C_2D_5OD solutions were measured at 313.2 K over the pressure range up to $\sim$6 MPa. The rotational correlation times, τ_r, of the CD and OD axes within CD_3OD and C_2D_5OD molecules and the CO axis within the CO_2 molecule were determined from $T_1(^2\text{H})$ and $T_1(^{17}\text{O})$, and the magnetic susceptibility-corrected chemical shifts, δ_{corr}, were derived from $\delta(^2\text{H})$. The differences in τ_r and δ_{corr} observed between the two alcohol systems: τ_r and δ_{corr} of OD in C_2D_5OD, decreased rapidly with increasing CO_2 concentration, while those of OD in CD_3OD remained almost unchanged at mole fractions of CO_2, x_{CO_2}, lower than $\sim$0.25 and then slightly decreased at higher x_{CO_2}. The hydrogen bonding structure in C_2D_5OD was found to be gradually broken down by CO_2 dissolution. On the other hand, in CD_3OD, it has been revealed that the hydrogen bonding structure can persist at $x_{CO_2} < \sim 0.25$ but then collapses at higher x_{CO_2}.

Keywords NMR · CO_2 · Alcohols · Chemical shifts · Relaxation times · Rotational correlation times

Electronic supplementary material The online version of this article (doi:10.1007/s10953-014-0222-z) contains supplementary material, which is available to authorized users.

T. Umecky (✉) · T. Takamuku
Graduate School of Science and Engineering, Saga University, Honjo-machi, Saga 840-8502, Japan
e-mail: umecky@cc.saga-u.ac.jp

T. Aida · T. Makino · T. Aizawa · M. Kanakubo (✉)
National Institute of Advanced Industrial Science and Technology, 4-2-1 Nigatake, Miyagino-ku, Sendai 983-8551, Japan
e-mail: m-kanakubo@aist.go.jp

1 Introduction

Gas-expanded liquid systems are composed of condensed gases and organic solvents [1]. In recent years, they have been of growing importance in fractionation, particle formation, polymerization, and chemical reaction processes [2]. CO_2 is one of the promising condensable gases because it is nonflammable, nontoxic, and inexpensive. An understanding of the fundamental nature of CO_2-expanded liquids is imperative to take advantage of the systems under optimum conditions for some intended uses.

Alcohols are the most commonly studied organic solvents in CO_2-expanded systems. There have been some reports on viscosities and volumetric properties for CO_2-expanded alcohols. Foster et al. have measured the viscosities of CO_2-expanded methanol and ethanol [3, 4]. The viscosities of the liquid phases decrease remarkably as CO_2 is dissolved in alcohols. Aizawa et al. have precisely determined the densities of various alcohols saturated with CO_2 [5]. They found that the liquid phases become denser at low CO_2 concentrations. The pressure (dissolution) effect leads to the viscosity decrease and density increase of the liquid phases in CO_2-expanded alcohol systems, though, in the single-component system consisting of either CO_2 or alcohol, the pressure (compression) straightforwardly enhances the viscosity with an increase of density. It is necessary and important to understand CO_2's role in expanded alcohols from a microscopic as well as a macroscopic viewpoint. As far as we know, there is no experimental study, in spite of some simulation work [5, 6], on microscopic properties such as solution structures and molecular motions in CO_2-expanded alcohols.

NMR spectroscopy is applicable to a wide range of substances because most organic and inorganic compounds contain NMR active nuclei. Moreover, NMR can independently provide some information about solvation structures, rotational motions, and translational diffusions from solvent-induced chemical shifts, relaxation times, and pulsed field gradient measurements. We have investigated the solvation structures of fluorinated compounds and the rotational dynamics of β-diketonato metal complexes in sub- and supercritical CO_2 [7–12]. In this work, to understand how CO_2 molecules act in expanded alcohols at the molecular level, ^{2}H and ^{17}O NMR relaxation times, $T_1(^2\mathrm{H})$ and $T_1(^{17}\mathrm{O})$, and ^{2}H chemical shifts, $\delta(^2\mathrm{H})$, in CO_2-saturated CD_3OD and C_2D_5OD solutions were examined at 313.2 K and pressures up to $\sim$6 MPa.

2 Experimental

CD_3OD, C_2D_5OD, and CO_2 were purchased from Sigma–Aldrich (100 atom-%D), Isotec (99.5 atom %D), and Showa Tansan (>99.99 vol-%), respectively. These chemicals were used without further purification. A 0.77 cm^3 sample of perdeuterated alcohol was carefully injected into a high-pressure NMR cell (6.0 mmϕ i.d., 10.0 mmϕ o.d.), and then a sealed capillary tube of C_6D_6 was inserted into the cell, which was used as an NMR lock solvent as well as external reference. Air containing paramagnetic oxygen in the high-pressure cell and line was carefully replaced several times by CO_2 gas at a low pressure. After ejecting the air sufficiently, NMR measurements were carried out under CO_2. Then, CO_2 was successively compressed into the cell at desired pressures. Absolute pressures were monitored with a precise digital indicator (Druck, DPI145) that had been traceably calibrated. To attain vapor–liquid equilibria, alcohols were first pressurized and mixed with CO_2 outside the superconducting magnet, and then inserted into the NMR probe at 313.2 K. The CO_2–alcohol systems were allowed to stand for $\sim$120 h below 2 MPa,

$\sim$70 h at 3 and 4 MPa, and $\sim$50 h above 5 MPa until the pressure drop became negligible, because the sample solution in the high-pressure cell cannot be agitated in the NMR probe.

All NMR spectra were recorded using a Varian Inova 500 FT-NMR spectrometer, where the resonance frequencies of ^{2}H and ^{17}O were 76.73 and 67.75 MHz, respectively. T_1 and δ values were repeatedly measured five times or more by a standard inversion-recovery and single pulse sequences, respectively. The numbers of accumulation times were fixed at 4 for ^{2}H and 128 for ^{17}O.

3 Results and Discussion

3.1 NMR Relaxation Times

The T_1s of quadrupolar nuclei such as ^{2}H and ^{17}O can be directly related to the rotational correlation time, τ_r, for the principal axis of the electric field gradient under the extreme narrowing condition that is satisfied throughout in the present systems as follows:

$$\frac{1}{T_1} = \frac{3\pi^2}{10}\frac{2I+3}{I^2(2I-1)}\left(1+\frac{\eta_q^2}{3}\right)\left(\frac{eQq}{h}\right)^2\tau_r. \quad (1)$$

Here, I is the spin quantum number, η_q is the asymmetry parameter, and eQq/h is the quadrupole coupling constant. The principal axes of the electric field gradients for the observed nuclei in CD_3OD, C_2D_5OD, and CO_2 are shown in Fig. 1. η_q is assumed to be negligible for all $T_1(^{2}H)$ and $T_1(^{17}O)$ in view of the high symmetry along the principal axes. The numerical data of $T_1(^{17}O)$ and $T_1(^{2}H)$ of alcohols and CO_2 are listed in the Supporting Information.

Figure 2 shows $1/T_1(^{2}H)$ and $1/T_1(^{17}O)$ of the hydroxy group in CD_3OD and C_2D_5OD as a function of CO_2 pressure. To make a direct comparison between $T_1(^{2}H)$ and $T_1(^{17}O)$, we have normalized $1/T_1(^{2}H)$ and $1/T_1(^{17}O)$ with the corresponding values $1/T_{1,0}$ at the atmospheric pressure. The $T_{1,0}/T_1$ values for ^{2}H and ^{17}O nuclei in both CD_3OD and C_2D_5OD change in a similar way with increasing CO_2 pressure. This strongly suggests that

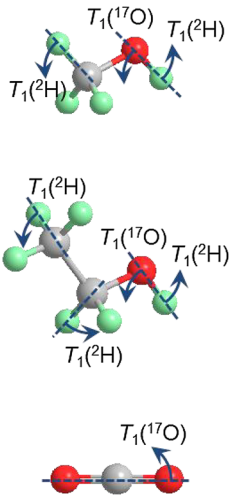

Fig. 1 Principal axes of τ_r responsible for $T_1(^{2}H)$ and $T_1(^{17}O)$ in alcohol and CO_2 molecules

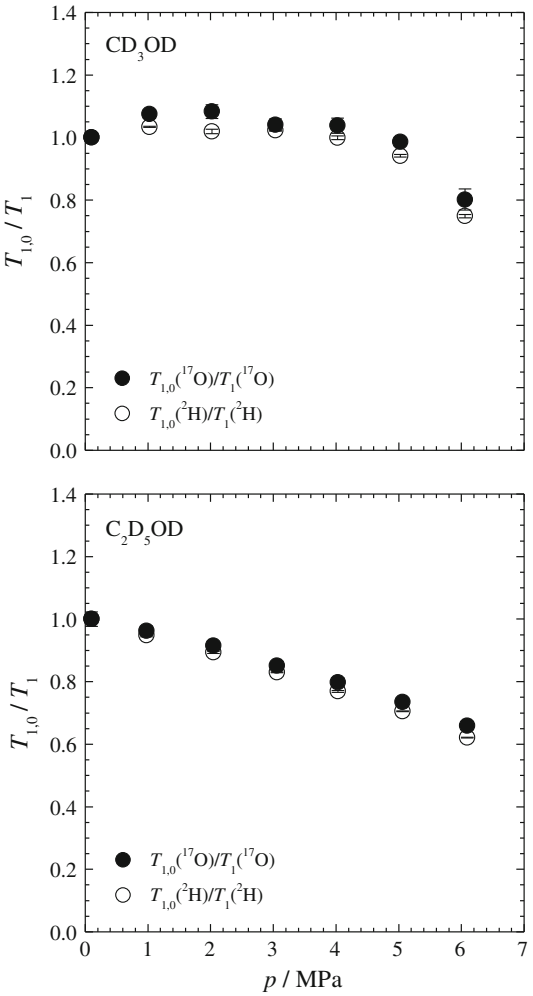

Fig. 2 Pressure dependence of normalized relaxation rates $T_{1,0}(^2H)/T_1(^2H)$ and $T_{1,0}(^{17}O)/T_1(^{17}O)$ of the hydroxy group of CD_3OD and C_2D_5OD. The *error bars* represent the standard deviations determined from five measurements

the change in $T_1(^2H)$ and $T_1(^{17}O)$ results from τ_r of the OD vector because eQq/h is predominantly determined by the intramolecular structures even if CO_2 is dissolved. In fact, Ikeda et al. have successfully obtained τ_r from $T_1(^2H)$ in several alcohols including CD_3OD and C_2D_5OD over a wide range of temperature and pressure with $eQq/h = 170$ kHz for the CD_3 and CD_2 groups of CD_3OD and C_2D_5OD molecules, 211 kHz for the OD group of CD_3OD, and 181 kHz for the OD group of C_2D_5OD [13]. In the present study, we determine τ_r of the CD_3, CD_2, OD vectors of CD_3OD and C_2D_5OD molecules from $T_1(^2H)$ in a similar manner by assuming that eQq/h is independent of CO_2 dissolution; however, τ_r of the OD vectors of CD_3OD and C_2D_5OD molecules cannot be obtained from $T_1(^{17}O)$ for lack of eQq/h for ^{17}O in the literature. On the other hand, τ_r of the CO vector of the CO_2 molecule is determined from $T_1(^{17}O)$ with $eQq/h = -3.92$ MHz, as in our previous report [11].

The τ_r values thus determined by the NMR experiments are plotted against x_{CO_2} in Fig. 3 for alcohols and Fig. 4 for CO_2. The relatively fast rotational motions (i.e., small τ_r)

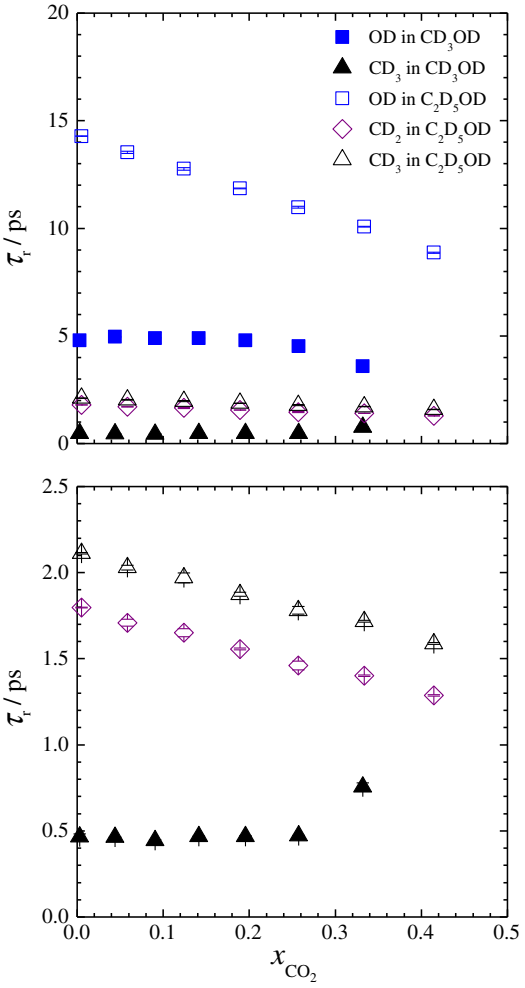

Fig. 3 Plots of τ_r of the OD, CD_2, and CD_3 groups of CD_3OD and C_2D_5OD against x_{CO_2} obtained by NMR experiments (*upper*). The range of $\tau_r < 2.5$ ps is magnified in the *lower panel*. The *error bars* represent the standard deviations determined from five measurements

of CD_2 and CD_3 in CD_3OD and C_2D_5OD are not strongly affected by CO_2 addition. On the other hand, τ_r of OD in C_2D_5OD significantly decreases with increasing x_{CO_2}, though τ_r of OD in CD_3OD shows different behavior; τ_r remains unchanged at low x_{CO_2} below $\sim$0.25 and then slightly decreases. Moreover, as is seen from Fig. 4, τ_r of CO_2 dissolved in CD_3OD and C_2D_5OD appreciably decreases with increasing x_{CO_2} despite the fast rotations. Unlike τ_r of OD, the change in τ_r of CO_2 in CD_3OD is more remarkable than that in C_2D_5OD. These results are discussed in the following section in terms of the hydrogen bonding structure and intermolecular interactions between alcohols and CO_2.

We also obtain τ_r of OH and τ_r of CO_2 in CH_3OH and C_2H_5OH saturated with CO_2 as a function of pressure by reanalyzing the previous MD simulation results [5]. It is noted that τ_r of CH_2 and CH_3 are unavailable because we have fixed the rotation of the alkyl substituents in the simulations. Although the simulation τ_r values are larger than the present experimental ones ($\sim$2 times for τ_r of the hydroxyl group and $\sim$1.2 for τ_r of CO_2), the concentration dependence of the τ_r values obtained by the simulations qualitatively

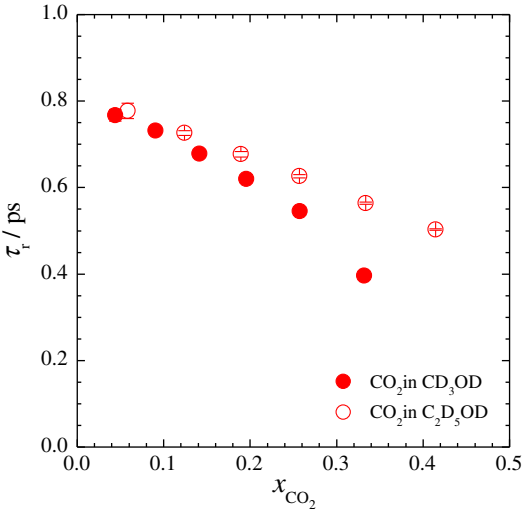

Fig. 4 Plots of τ_r of CO_2 against x_{CO_2} obtained by NMR experiments. The *error bars* represent the standard deviations determined from five measurements

reproduces the trends of the experimental values against the CO_2 pressure (see Fig. 5). The mechanism of CO_2 dissolution in alcohols is discussed in the later section on the basis of both NMR experimental and MD simulation results.

3.2 Viscosity Dependence of the Rotational Correlation Times

In a liquid, the rotational motion of a molecule can be described by the Debye diffusion model, where a molecule rotates with a small step angular random walk [14]. Frequently, τ_r is related to the macroscopic viscosity, η, and the thermodynamic temperature, T:

$$\tau_r = a\frac{\eta}{T} + b, \tag{2}$$

where a and b are coefficients that can be experimentally determined. In the well-known Stokes–Einstein–Debye equation, a and b are replaced by V/k_B and zero, respectively, where V is the volume of a spherical rotator. The plots of τ_r against η/T are given in Fig. 6 for the CD_3, CD_2, and OD vectors in alcohols and Fig. 7 for the CO vector in CO_2. It is noted that η of non-deuterated alcohols (CH_3OH and C_2H_5OH) saturated with CO_2 were interpolated from the literature data [3, 4]. Table 1 lists the coefficients a and b obtained by the least-square fittings. The τ_r value of OD is found to be much more sensitive to η than those of CD_3 and CD_2. The very small η effect is similarly observed for the hindered rotation of the alkyl groups. Meanwhile, τ_r of CO_2 in CD_3OD and C_2D_5OD linearly increases with η/T, showing that η is still responsible for the rotational motion of CO_2 molecules. Moreover, Fig. 7 shows that at $\eta/T > \sim 8$, i.e., below the CO_2 pressure of 5 MPa, τ_r for CO_2 in CD_3OD is much larger than that in C_2D_5OD. This means that the rotational motion of CO_2 is slower in CD_3OD than in C_2D_5OD in dilute solutions of CO_2 whereas the difference should disappear at higher CO_2 concentrations.

3.3 NMR Chemical Shifts

The observed CO_2-induced chemical shifts (δ_{obs}) involve all the solvent effects, which can be separated into two contributions from intermolecular interactions and magnetic

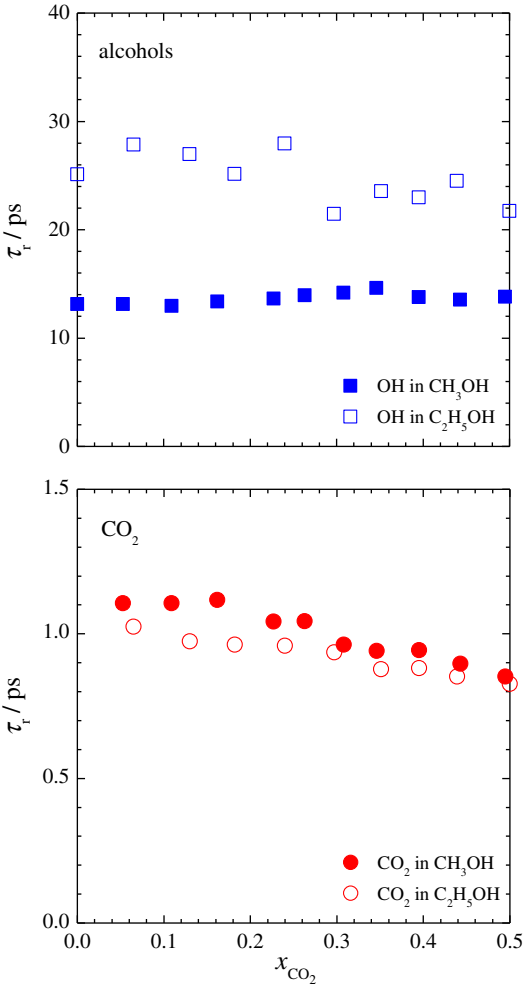

Fig. 5 Plots of τ_r for the OH group of alcohols and CO_2 in CH_3OH and C_2H_5OH systems against x_{CO_2}, obtained by MD simulations

susceptibility changes. We can obtain the magnetic susceptibility-corrected chemical shift, δ_{corr}, from:

$$\delta_{corr} = \delta_{obs} - \frac{4\pi}{3}\chi_{v,sam} = \delta_{obs} - \frac{4\pi}{3}\left(\frac{\rho}{M}\chi_{m,sam}\right) \times 10^6. \quad (3)$$

Here, $\chi_{v,sam}$ and $\chi_{m,sam}$ are the volume and molar magnetic susceptibilities, respectively. ρ and M denote the density and averaged molar mass of the sample mixture, respectively, which are calculated from $pVTx$ relations using Peng–Robinson equation of state. The values of $\chi_{m,sam}$ for CO_2–alcohol mixtures are estimated as:

$$\chi_{m,sam} = x_{alcohol}\chi_{m,alcohol} + x_{CO_2}\chi_{m,CO_2}. \quad (4)$$

The above estimation was successfully applied to water–alcohol mixtures [15]. χ_m for normal alcohols were used because χ_m for deuterated ones are unavailable. This is a reasonable approximation in view of small difference of χ_m between deuterated and non-

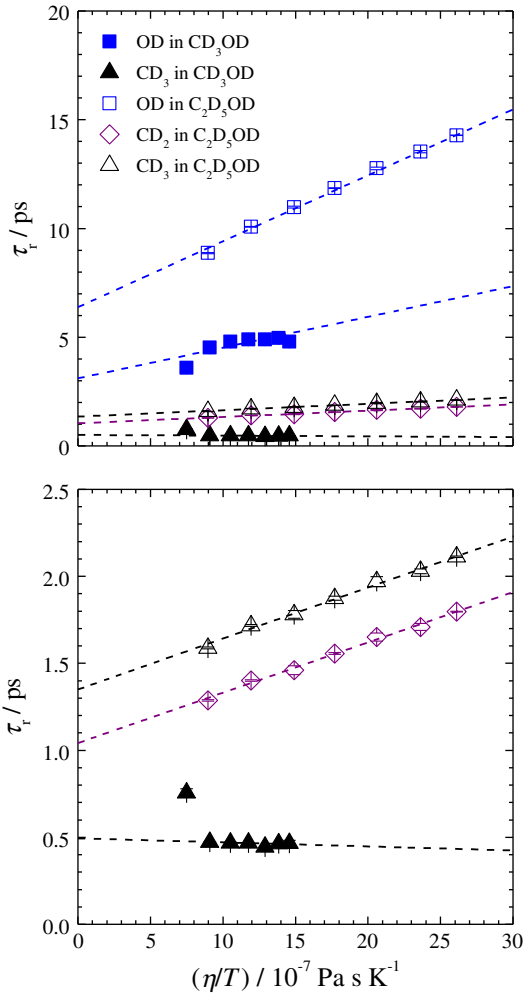

Fig. 6 Plots of τ_r of the OD, CD_2, and CD_3 groups of CD_3OD and C_2D_5OD against η/T (*upper*). The *broken lines* are given by the linear regressions of the experimental data through Eq. 2. The range of $\tau_r < 2.5$ ps is magnified in the *lower panel*. The *error bars* represent the standard deviations determined from five measurements

deuterated solvents such as in chloroform, cyclohexane, and benzene [16]. In the present analyses, we have employed $\chi_m = -21.4 \times 10^{-6}$ for CH_3OH, -33.7×10^{-6} for C_2H_5OH, and -21.0×10^{-6} $cm^3 \cdot mol^{-1}$ for CO_2 [17]. In the composition range studied, the susceptibility correction term, $-4\pi\chi_{v,sam}/3$, in Eq. 3 increases to 0.09 ppm for the CD_3OD system and decreases to 0.05 ppm for the C_2D_5OD system.

The concentration dependence of δ_{corr} is given in Fig. 8, where δ_{corr} was scaled in reference to the chemical shift under the atmospheric pressure, $\delta_{corr,0}$. In the C_2D_5OD system, the $\delta_{corr} - \delta_{corr,0}$ value of the OD group gradually decreases with increasing x_{CO_2}, whereas the value of the CD_3 and CD_2 groups slightly increases to $\sim$0.1 ppm in the composition range studied. The negative change in $\delta_{corr} - \delta_{corr,0}$ of OD is caused by the breakdown of hydrogen bonding between the hydroxyl groups. The slight positive changes in $\delta_{corr} - \delta_{corr,0}$ of the alkyl groups are attributable to the rise of other intermolecular interactions since the breakdown of hydrogen bonding affects δ_{corr} of the alkyl groups less as observed in neat methanol and ethanol over a wide range of temperature and pressure

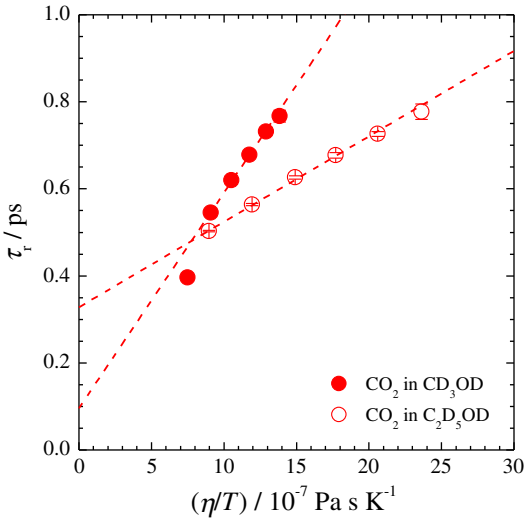

Fig. 7 Plots of τ_r of CO_2 against η/T. The *broken lines* are given by the linear regressions of the experimental data through Eq. 2. The *error bars* represent the standard deviations determined from five measurements

Table 1 Coefficients a and b in Eq. 2 obtained by least-squares fittings

Alcohol systems	a (10^{-7} Pa^{-1}·K)	b (ps)
CD_3OD		
–OD	7.01	4.02
$–CD_3$	−0.23	0.49
CO_2	4.95	0.10
C_2D_5OD		
–OD	30.32	6.38
$–CD_2–$	2.89	1.04
$–CD_3$	2.93	1.35
CO_2	1.96	0.33

[13]. In the CD_3OD system, the $\delta_{corr} - \delta_{corr,0}$ value of the OD group remains virtually unchanged at lower x_{CO_2} up to ∼0.25 and then decreases at higher x_{CO_2}, whereas the value of CD_3 shows a remarkable increase to ∼0.4 ppm in the composition range studied. The lack of change in $\delta_{corr} - \delta_{corr,0}$ of OD indicates that the hydrogen bonding structure persists at lower x_{CO_2}. The discrepancy between CD_3OD and C_2D_5OD can be interpreted as the difference in the strength of hydrogen bonding, $CD_3OD > C_2D_5OD$.

3.4 Mechanism of CO_2 Dissolution in Alcohols

On the basis of the present experimental results together with the previous MD simulations, a feasible model for CO_2 dissolution in alcohols may be proposed. As shown in Figs. 3 and 8, τ_r and $\delta_{corr} - \delta_{corr,0}$ of OD in C_2D_5OD decreases with increasing x_{CO_2}, while τ_r and $\delta_{corr} - \delta_{corr,0}$ of OD in CD_3OD remains unchanged at low x_{CO_2} below ∼0.25 and then slightly decreases. Both decreases in τ_r and $\delta_{corr} - \delta_{corr,0}$ of OD indicate the breakdown of the hydrogen bonding; i.e., the rotational motion of OD is enhanced and the shielding constant of OD is increased by CO_2 dissolution. Moreover, Fig. 7 shows that the rotational

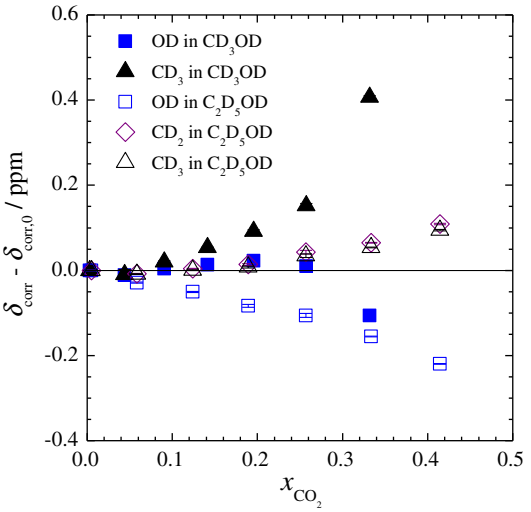

Fig. 8 Plots of ^{2}H chemical shift ($\delta_{corr} - \delta_{corr,0}$) of the OD, CD_2, and CD_3 groups of CD_3OD and C_2D_5OD against x_{CO_2}. The *error bars* represent the standard deviations determined from five measurements

motion of CO_2 in CD_3OD is slower than that in C_2D_5OD at the same viscosities, suggesting the stronger interactions of CO_2 with CD_3OD despite the persistence of the more stable hydrogen bonding structure in methanol. These results imply that CO_2 molecules are dissolved into the polar space in alcohols produced by the hydrogen bonding structure, and dissolved CO_2 destroys the relatively weaker hydrogen bonding structure in ethanol but not in methanol at low x_{CO_2}. Further addition of CO_2 in alcohols promotes the breakdown of the hydrogen bonding structure, which could concurrently result in aggregation among the alkyl groups as suggested by the increase in $\delta_{corr} - \delta_{corr,0}$ of the alkyl groups.

4 Conclusion

We have measured $T_1(^2H, ^{17}O)$ and $\delta(^2H)$ in the CO_2-saturated CD_3OD and C_2D_5OD solutions at 313.2 K in the pressure range up to $\sim$6 MPa. The τ_r values of alcohols and CO_2 estimated from the T_1 values were discussed in terms of intermolecular interactions. Moreover, after the magnetic susceptibility correction, the δ_{corr} values were interpreted in relation to the hydrogen bonding structure. The hydrogen bonding structure in the ethanol–CO_2 system is gradually broken down with increasing x_{CO_2}. On the other hand, the structure in the methanol–CO_2 system can be held in the range of $x_{CO_2} < \sim 0.25$; however, further increase in CO_2 leads to the disruption of the hydrogen bonding structure in methanol in a similar manner to that in ethanol.

References

1. Akien, G.R., Poliakoff, M.: A critical look at reactions in class I and II gas-expanded liquids using CO2 and other gases. Green Chem. **11**, 1083–1100 (2009)
2. Hutchenson, K.W., Scurto, A.M., Subramaniam, B. (eds.): Gas-Expanded Liquids and Near-Critical Media, ACS Symposium Series 1006. American Chemical Society, Washington, DC (2009)
3. Sih, R., Dehghani, F., Foster, N.R.: Viscosity measurements on gas expanded liquid systems–methanol and carbon dioxide. J. Supercrit. Fluids **41**, 148–157 (2007)
4. Sih, R., Armenti, M., Mammucatri, R., Dehghani, F., Foster, N.R.: Viscosity measurements on saturated gas expanded liquid systems–ethanol and carbon dioxide. J. Supercrit. Fluids **43**, 460–468 (2008)

5. Aida, T., Aizawa, T., Kanakubo, M., Nanjo, H.: Relation between volume expansion and hydrogen bond networks for CO_2–alcohol mixtures at 40°C. J. Phys. Chem. B **114**, 13628–13636 (2010)
6. Saharay, M., Balasubramanian, S.: Electron donor-acceptor interactions in ethanol–CO_2 mixtures: an ab initio molecular dynamics study of supercritical carbon dioxide. J. Phys. Chem. B **110**, 3782–3790 (2006)
7. Kanakubo, M., Umecky, T., Kawanami, H., Aizawa, T., Ikushima, Y., Masuda, Y.: Determination of anisotropic solvation structure of octafluorotoluene in supercritical carbon dioxide by means of solvent-induced ^{19}F NMR chemical shift. Chem. Phys. Lett. **338**, 95–100 (2001)
8. Kanakubo, M., Umecky, T., Liew, C.C., Aizawa, T., Hatakeda, K., Ikushima, Y.: High-pressure NMR studies on solvation structure in supercritical carbon dioxide. Fluid Phase Equilib. **194–197**, 859–868 (2002)
9. Kanakubo, M., Umecky, T., Raveendran, P., Ebina, T., Ikushima, Y.: High-pressure ^{19}F NMR measurements of a series of fluorinated benzenes in supercritical carbon dioxide. J. Solution Chem. **33**, 863–874 (2004)
10. Umecky, T., Kanakubo, M., Ikushima, Y.: ^{9}Be NMR relaxation measurements of bis(acetylacetonato)beryllium(II) in liquid and supercritical carbon dioxide: a clear evidence of near-critical solvation effect on rotational correlation time. J. Phys. Chem. B **106**, 11114–11119 (2002)
11. Umecky, T., Kanakubo, M., Ikushima, Y.: Experimental determination of reorientational correlation time of CO_2 over a wide range of density and temperature. J. Phys. Chem. B **107**, 12003–12008 (2003)
12. Umecky, T., Kanakubo, M., Ikushima, Y.: Fluorination effect on rotational correlation times of tris(β-diketonato)aluminum(III) in CO_2 by ^{27}Al NMR relaxation measurements. J. Phys. Chem. B **115**, 10622–10630 (2011)
13. Tsukahara, T., Harada, M., Tomiyasu, H., Ikeda, Y.: NMR studies on effects of temperature, pressure, and fluorination on structures and dynamics of alcohols in liquid and supercritical states. J. Phys. Chem. A **112**, 9657–9664 (2008)
14. Debye, P.: Polar Molecules. Dover, New York (1929)
15. Mizuno, K., Ochi, T., Shimada, S., Nishimura, Y., Maeda, S., Koga, Y.: Magnetic susceptibility of aqueous *tert*-butanol. Phys. Chem. Chem. Phys. **1**, 133–135 (1999)
16. Mizuno, K., Tamiya, Y., Mekata, M.: External double reference method to study concentration and temperature dependences of chemical shifts determined on a unified scale. Pure Appl. Chem. **76**, 105–114 (2004)
17. Lide, D.R. (ed.): CRC Handbook of Chemistry and Physics, 86th edn. CRC Press, Boca Raton (2005)